Thermal Decomposition Pathways and Rates for Dimethylaluminum Hydride

Stephen P. Walch* and Christopher E. Dateo

Eloret Corporation, MS 230-3, NASA Ames Research Center, Moffett Field, California 94035-1000

Received: November 17, 2000; In Final Form: March 6, 2001

Calculations have been carried out for the thermal decomposition of dimethylaluminum hydride (DMAlH). For each decomposition pathway, the stationary point geometries and harmonic frequencies were characterized using complete active space self-consistent field (CASSCF)/derivative methods and the correlation consistent polarized valence double-ζ (cc-pVDZ) basis set. Accurate energetics were obtained by combining the coupled cluster singles and doubles with perturbational estimate of triples [CCSD(T)] results using the cc-pVTZ basis set with an extrapolation to the basis set limit using the cc-pVDZ, cc-pVTZ, and cc-pVQZ basis sets at the Moller−Plesset second-order perturbation theory (MP2) level. The geometries, energetics, and harmonic frequencies were used to obtain rate constants using conventional transition state theory. It was found that the lowest energy pathway leads to $CH_3AlCH_2 + H_2$ with a barrier of 71.1 kcal/mol, which is below the first product resulting from direct bond breaking ($CH_3Al + CH_3$ at 82.2 kcal/mol). Decomposition of DMAlH dimer was also considered. The rate-limiting step here is elimination of H_2 from the DMAlH dimer, and the best estimate of the barrier for this process is 80 kcal/mol [from CCSD(T) calculations with the cc-pVDZ basis set]. This barrier is too large for this pathway to play a major role in Al chemical vapor deposition.

I. Introduction

Dimethylaluminum hydride (DMAlH) is a commonly used precursor to deposit aluminum by chemical vapor deposition (CVD) for integrated circuit applications. Understanding of growth mechanisms is key to process development and control. In the case of DMAlH, this process is not well understood. The two main possibilities are (i) that DMAlH decomposes in the gas phase (either from the monomer or dimer) to give reactive species which subsequently react with the surface and (ii) that DMAlH reacts directly with the surface in a gas−surface reaction. In a recent paper, Nakajima and Yamashita[1] used ab initio molecular orbital methods [MP2 and density functional theory (DFT)] to study gas-phase decomposition reactions. These authors studied bond-breaking processes in DMAlH and also looked at bimolecular processes in which two DMAlH molecules split off CH_4, C_2H_6, and H_2, respectively. In addition, they computed the equilibrium concentration of the DMAlH dimer and trimer as a function of temperature. They concluded that the barriers for bond-breaking processes from the monomer are too large for these processes to be important. However, we show in the present study that the decomposition of DMAlH to $CH_3AlCH_2 + H_2$ has a lower barrier than simple bond-breaking processes, and this channel was not considered in their work. They did find low-energy pathways for bimolecular processes. In particular, two DMAlH molecules going to $(CH_3)_2Al-AlCH_3H + CH_4$ and $(CH_3)_2Al-Al(CH_3)_2 + H_2$ have low barriers, 28 and 22 kcal/mol, respectively. They computed a binding energy of ∼32 kcal/mol for the DMAlH dimer. Their calculations show mostly dimer in the equilibrium gas-phase mixture at temperatures <273 K but mostly monomer at temperatures >673 K.

Other workers have studied the DMAlH dimer. Hiraoka and Mashita[2] found a binding energy of 32 kcal/mol using the MP2 method. Willis and Jensen[3] studied convergence of the dimerization energy using ab initio and DFT methods. They found that DFT underestimates the binding energy but that hybrid functionals such as B3LYP[4] work better than other functionals. Tachibana, Sakato, and Omato[5] also studied the reactivity of DMAlH with an H-terminated Si surface using six model reactions.

In this paper, we present results for the thermal decomposition of DMAlH using highly accurate ab initio methods. Section II discusses the computational details, section III discusses the results, and the conclusions are presented in section IV.

II. Calculational Details

The geometries and harmonic frequencies for all of the stationary points (minima or saddle points) were determined using the complete active space self-consistent field (CASSCF)/derivative method with the correlation consistent polarized valence double-ζ (cc-pVDZ) basis sets.[6] In these calculations three bond pairs were included in the active space. These bond pairs are the AlH and two $AlCH_3$ bonds, and the active space consists of six electrons distributed over six orbitals. The energetics were obtained using the coupled cluster single and double excitation with perturbational estimate of triple excitations [CCSD(T)] method using the cc-pVTZ basis set and extrapolated to the complete basis set (CBS) limit using the Moller−Plesset second-order perturbation theory method (MP2) with the cc-pVDZ, cc-pVTZ, and cc-pVQZ basis sets.[7] [The CCSD(T) and MP2 calculations made use of the closed shell methods[8] for singlet states and open shell methods[9] for cases with open shells.] The MP2 results were extrapolated to the basis set limit using the Martin−Schwartz three-point extrapolation.[10] The results of the MP2 extrapolation were combined with CCSD(T) results obtained with the cc-pVTZ basis set to obtain an estimate of the CCSD(T) results in the limit of a complete basis set. The basis for this was described by Ricca and Bauschlicher,[11] who noticed that for bond strengths the ratio D_e[CCSD(T)]/D_e[MP2] was constant for a series of correlation consistent basis sets. Thus, for barrier heights and other relative

10.1021/jp0042462 CCC: $20.00
Published on Web 05/03/2001

TABLE 1: AlH Bond Strength Calculation[a]

cc-pVDZ	cc-pVTZ	cc-pVQZ	CBS	D_e,[b] kcal/mol
		AlH		
−242.52850	−242.54552	−242.54983	−242.5525	73.6
		Al		
−241.92124	−241.93117	−241.93366	−241.9352	
		H		
−0.49928	−0.49981	−0.49995	−0.5000	
a-cc-pVDZ	**a-cc-pVTZ**	**a-cc-pVQZ**	**CBS**	**D_e,[b] kcal/mol**
		AlH		
−242.53193	−242.54648	−242.55016	−242.5524	73.7
		Al		
−241.92266	−241.93147	−241.93366	−241.9350	
		H		
−0.49933	−0.49982	−0.49995	−0.5000	

[a] CCSD(T) calculations at the CASSCF (cc-pVDZ) optimal geometry (3.186 au). [b] Experiment 73.1 kcal/mol (ref 20).

energy quantities, the value in the limit of a complete basis set was obtained as

$$\{\Delta E[\text{cc-pVTZ/CCSD(T)}]/\Delta E[\text{cc-pVTZ/MP2}]\}\Delta E[\text{CBS/MP2}] \quad (1)$$

where ΔE[cc-pVTZ /CCSD(T)] and ΔE[cc-pVTZ /MP2] are the values obtained with the cc-pVTZ basis set for CCSD(T) and MP2, respectively, and ΔE[CBS/MP2] is the MP2 value extrapolated to the CBS limit. In these calculations the 10 electron Ne core of the Al atom was not correlated.

Tests of the MP2 extrapolation have been made by Dunning and Peterson.[12] They studied convergence of MP2 and MP3 extrapolation of CCSD(T) results for a series of diatomic molecules formed from first-row atoms. They found the MP3 extrapolation was more accurate than the MP2 extrapolation. However, for AB molecules MP2 extrapolation of a-cc-pVTZ results leads to an average error in D_e of 0.72 kcal/mol. It is probable that D_e is a more difficult quantity to compute than barrier heights. Thus, their work suggests our results should be good to well within 1 kcal/mol.

Calculations were also carried out using the internally contracted configuration interaction (ICCI) method.[13] These calculations used the same active space of six electrons in six orbitals and made use of a selected reference list consisting of configurations with CI coefficients >0.05. Here we included a multireference analogue of the Davidson correction,[14] and this is denoted by ICCI +Q.

The pathways for thermal decomposition of the DMAlH dimer were studied using the density functional theory (DFT) method with the B3LYP functional and the 6-31G basis set.

For the reactions with barriers, rate coefficients as a function of temperature were obtained using conventional transition state theory. For reactions without barriers (e.g., $CH_3AlH + CH_3$) a Gorin-like model was used.

The CASSSCF/derivative calculations were carried out using DALTON,[15] the CCSD(T) and ICCI calculations were carried out using MOLPRO,[16] and the MP2 calculations were done using Gaussian94.[17] The transition state theory calculations[18] were carried out using POLYRATE.[19]

III. Discussion

Table 1 shows the results of CCSD(T) calculations for the D_e of the $^1\Sigma^+$ state of AlH. In the case of Si and Cl we found that the augmented correlation consistent polarized valence n zeta (a-cc-pVnZ) basis sets gave results that were significantly different from those obtained with the cc-pVnZ basis sets. However, for Al the results in Table 1 are nearly identical for the augmented and unaugmented basis sets. This is particularly true of the results that are extrapolated to the CBS limit. On this basis we chose to use the unaugmented correlation consistent basis sets in these calculations. The D_e of AlH obtained by extrapolation with the cc-pVnZ basis set is 73.6 kcal/mol compared to an experimental value of 73.1 kcal/mol.[20]

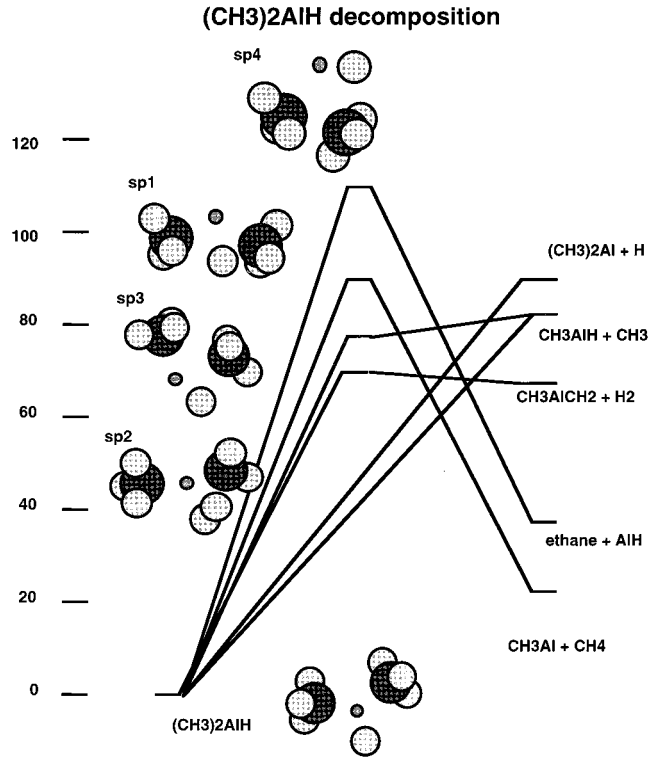

Figure 1. Energetics for the thermal decomposition of DMAlH. The lowest energy pathway (through sp3) is to $CH_3AlCH_2 + H_2$. This pathway has a lower barrier than dissociation of an Al−C bond (leading to $CH_3AlH + CH_3$).

Figure 1 shows saddle point structures and energetics for the thermal decomposition of DMAlH. Table 2 gives relative energies for each of the stationary points for this system with respect to $(CH_3)_2AlH$. The results given in Table 2 include CCSD(T) results for the cc-pVDZ and cc-pVTZ basis sets, MP2 results for the cc-pVDZ, cc-pVTZ, and cc-pVQZ basis sets, and extrapolated values to the CBS limit. The extrapolated MP2 results were combined with the CCSD(T) results with the cc-pVTZ basis using eq 1 to give the values in the column "CBS from MP2" in Table 2. These energetics along with the CASSCF harmonic frequencies were used in the conventional transition state theory calculations of the rate coefficients as a function of temperature.

Figure 1 shows the four saddle points that were characterized in this work. The lowest energy pathway leads to $CH_3AlCH_2 + H_2$ and has a barrier of 71.1 kcal/mol. The next highest pathway leads to $CH_3AlH + CH_3$ and is a barrierless process other than the exoergicity of 82.2 kcal/mol. The third pathway leads to $CH_3Al + CH_4$ and has a barrier of 90.4 kcal/mol. This pathway in the reverse direction corresponds to the addition of CH_3Al to CH_4, which is formally a carbene addition process. However, the excitation energy from the $^1\Sigma^+$ ground state to the $^3\Pi$ excited state state of AlH is computed to be 43.3 kcal/mol; thus, a high barrier is expected (vide infra). Finally, the highest energy saddle point in Figure 1 leads to ethane plus

TABLE 2: Energy Differences (Kilocalories per Mole) for Thermal Decomposition of DMAlH

CCSD(T)

structure	cc-pVDZ	cc-pVTZ	CBS from mp2
$(CH_3)_2Al + H$	83.8	87.2	89.5
$CH_3AlH + CH_3$	78.8	83.5	82.2
sp4	103.1	108.6	110.7
sp1	86.8	89.0	90.4
sp2	72.8	72.0	71.1
sp3	74.3	77.0	77.3
$CH_3AlCH_2 + H_2$	65.9	67.4	67.5
ethane + AlH	25.5	33.8	36.6
$CH_3Al + CH_4$	15.7	20.4	22.8
$(CH_3)_2AlH$	0.0	0.0	0.0

MP2

structure	cc-pVDZ	cc-pVTZ	cc-pVQZ	CBS
$(CH_3)_2Al + H$	80.7	84.1	85.5	86.3
$CH_3AlH + CH_3$	81.2	85.7	87.3	84.4
sp4	117.4	120.9	122.3	123.2
sp1	94.0	94.9	95.7	96.4
sp2	73.9	72.5	72.0	71.6
sp3	80.3	81.2	81.4	81.5
$CH_3AlCH_2 + H_2$	68.3	68.9	69.0	69.0
ethane + AlH	31.5	38.3	40.3	41.5
$CH_3Al + CH_4$	20.3	23.7	25.4	26.5
$(CH_3)_2AlH$	0.0	0.0	0.0	0.0

TABLE 3: Relative Energies for $(CH_3)_2AlH$ Thermal Decomposition Based on ICCI +Q Calculations

structure	zero-point energy	ΔE,[a] kcal/mol
sp4	0.077371	107.9
$(CH_3)_2Al + H$	0.072602	83.2
$CH_3AlH + CH_3$	0.071985	77.7
sp2	0.074836	69.2
$CH_3AlCH_2 + H_2$	0.069581	60.6
sp1	0.078202	89.8
sp3	0.076944	75.6
ethane + AlH	0.081731	35.4
$CH_3Al + CH_4$	0.080332	22.8
$(CH_3)_2AlH$	0.079933	0.0

[a] Includes zero-point energy.

TABLE 4: Extrapolated Relative Energies (Kilocalories per Mole) for $(CH_3)_2AlH$ Thermal Decomposition Based on ICCI +Q Calculations

structure	cc-pVTZ	CBS from mp2
$(CH_3)_2Al + H$	87.8	90.1
$CH_3AlH + CH_3$	82.7	81.4
sp4	109.5	110.0
sp1	90.9	92.3
sp2	72.4	71.5
sp3	77.5	77.8
$CH_3AlCH_2 + H_2$	67.1	67.2
ethane + AlH	34.2	37.1
$CH_3Al + CH_4$	22.6	25.3
$(CH_3)_2AlH$	0.0	0.0

AlH and has a barrier of 110.7 kcal/mol. Only the first pathway leading to $CH_3AlCH_2 + H_2$ is below the energy of $CH_3AlH + CH_3$ (82.2 kcal/mol), which arises by simple dissociation of an Al−C bond. Similarly, the pathway leading to $CH_3Al + CH_4$ is slightly above the energy of $(CH_3)_2Al + H$ (89.5 kcal/mol) and it arises by simple dissociation of an Al−H bond. These results show that the most probable pathway based on energetics is to $CH_3AlCH_2 + H_2$.

Tables 3 and 4 show results for the thermal decomposition of DMAlH using the ICCI method. Table 3 gives the zero-point energy obtained from the CASSCF/derivative calculations and the relative energies (based on ICCI +Q results). Table 4 gives the ICCI relative energies with an MP2 extrapolation to the CBS limit. This is done using eq 1 but with the CCSD(T) energetics replaced by ICCI +Q energetics. From a comparison of Tables 2 and 4 it is seen that the relative energies agree to within 1 kcal/mol except for sp1 and $CH_3Al + CH_4$, which are higher by 1.9 and 2.5 kcal/mol for ICCI +Q than for CCSD(T), respectively. This good agreement gives us confidence in the CCSD(T) and ICCI +Q methods for this system.

TABLE 5: AlH−H_2 Relative Energies Based on ICCI +Q Calculations

structure	zero-point energy	ΔE,[a] kcal/mol
$AlH + H_2$	0.013203	0.0
sp1	0.016251	15.3
sp2	0.012434	36.6
AlH_3	0.017503	−26.0

[a] Including zero-point energy.

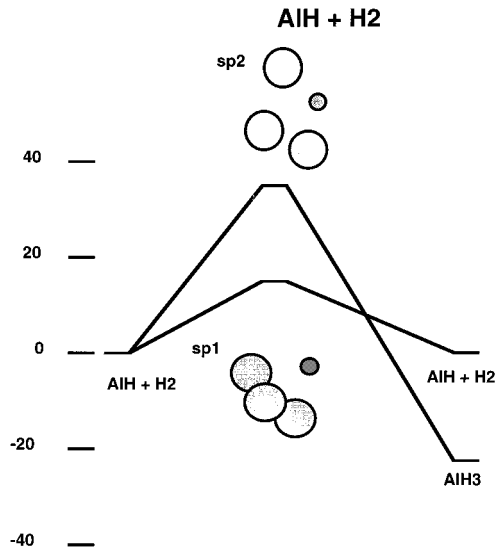

Figure 2. Energetics for the reaction of AlH with H_2. Sp1 is an exchange process, whereas sp2 is the addition process.

Table 5 and Figure 2 show results for the reaction of AlH with H_2. These calculations were carried out because there was some concern about the high barrier for sp1 for the DMAlH system. (Sp1 is the saddle point for the reverse of insertion of CH_3Al into CH_4.) Figure 2 shows the saddle point structures and energetics for this reaction. Here it is seen that the lower energy pathway is an exchange process, which interchanges H atoms via a symmetric saddle point. This process has a relatively low barrier of 15.3 kcal/mol. The higher energy pathway is the expected insertion of AlH into H_2 to give AlH_3. This process has a barrier of 36.6 kcal/mol. This barrier height based on the computed singlet−triplet separation of 43.3 kcal/mol for AlH is reasonable. As discussed elsewhere,[21] we have found a correlation between singlet−triplet separation in a carbene and reactivity; for example, for the reactions $SiH_2 + H_2$, $SiHCl + H_2$, and $SiCl_2 + H_2$ the singlet−triplet separations are 20.0, 33.9, and 53.4 kcal/mol and the barriers to insertion are 0.0, 15.3, and 37.8 kcal/mol, respectively. Thus, the barrier height obtained here for AlH inserting into H_2 is reasonable.

Calculations were also carried out for AlH plus CH_4. The results for this system are given in Table 6 and Figure 3. From Figure 3 it is seen that the lowest energy pathway is an exchange process that converts $CH_4 + AlH$ to $CH_3Al + H_2$ with a barrier of 31.4 kcal/mol. Two insertion processes were studied. Insertion of AlH into CH_4 has a barrier height of 50.3 kcal/mol, whereas insertion of CH_3Al into H_2 has a barrier height of 44.3 kcal/

TABLE 6: AlH−CH_4 Relative Energies Based on ICCI +Q Calculations

structure	zero-point energy	ΔE,[a] kcal/mol
CH3AlH +H	0.041506	59.8
sp3	0.045068	50.3
CH_3AlH_2	0.048579	−20.2
sp2	0.043721	51.5
$AlH_2 + CH_3$	0.037431	52.8
sp1p	0.048733	31.4
CH_3Al + H2	0.04371	0.8
sp1	0.044735	44.3
CH_4 + AlH	0.049825	0.0

[a] Includes zero-point energy.

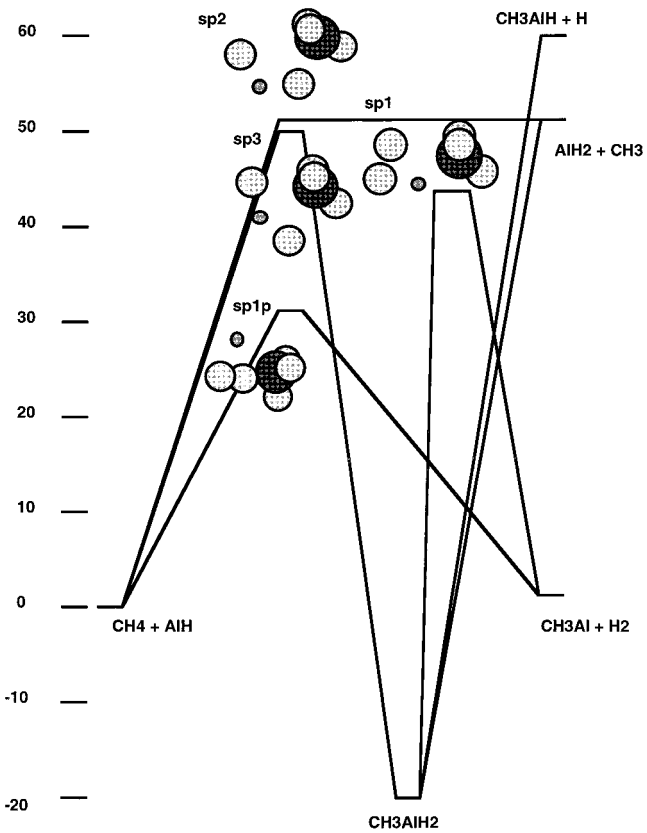

Figure 3. Energetics for the reaction of AlH with CH_4. Sp1p is an exchange saddle point (analagous to sp1 for AlH + H_2). Sp1 is a saddle point for CH_3Al adding to H_2. Sp3 is a saddle point for AlH adding to CH_4.

mol. The barrier height for CH_3Al inserting into CH_4 is 67.6 kcal/mol (see Table 2). Looking at the saddle point geometry for this process, it is seen that the Al end of CH_3Al is approaching the C end of the CH bond being inserted into. From Figure 3 it is seen that the saddle point for insertion of AlH into CH_4 has the Al end of AlH approaching the H end of the CH bond. It is probable that this orientation is much less favorable in the CH_3Al + CH_4 case due to steric interactions between the two CH_3 groups and this is what forces the reaction to proceed via the less favorable orientation where the Al approaches the C end of the CH bond. These considerations are consistent with a higher barrier in the CH_3Al + CH_4 case as compared to AlH + CH_4. An additional consideration from the AlH + H_2 and AlH + CH_4 systems is that there should be a symmetric exchange saddle point in the CH_3Al + CH_4 system. This saddle point has not been characterized; however, it is not relevant to the thermal decomposition of DMAlH.

TABLE 7: DMAlH Reaction Set High-Pressure TST Rate Coefficients

$$k(T) = A \exp(-E_a/kT)$$

reaction	σ[a]	A, s^{-1} or cm^3 $molecule^{-1}$ s^{-1}	E_a, kcal/mol
$(CH_3)_2AlH \rightarrow AlCH_3 + CH_4$	2	4.854×10^{12}	90.219
$AlCH_3 + CH_4 \rightarrow (CH_3)_2AlH$	3	1.111×10^{-10}	70.742
$(CH_3)_2AlH \rightarrow H_3CAlCH_2 + H_2$	6	5.218×10^{12}	68.845
$H_3CAlCH_2 + H_2 \rightarrow (CH_3)_2AlH$	2	5.675×10^{-11}	6.822
$(CH_3)_2AlH \rightarrow H_3CAlH + CH_3$	2	2.550×10^{13}	77.050
$H_3CAlH + CH_3 \rightarrow (CH_3)_2AlH$[b]	1	2.522×10^{-11}	0.253
$(CH_3)_2AlH \rightarrow AlH + C_2H_6$	2	3.107×10^{14}	107.933
$AlH + C_2H_6 \rightarrow (CH_3)_2AlH$	2	1.786×10^{-09}	77.321

[a] Reaction path degeneracy. [b] Loose transition states, treated with Gorin-like model.

TABLE 8: DFT Energy Differences (Kilocalories per Mole) for DMAlH Decomposition

structure	6-31G basis	6-31G** basis
$MAlCH_2 + H_2$	65.6	68.2
M_2AlH, sp2	93.0	87.6
M_2AlH	0.0	0.0

Table 7 shows computed rate constants for the decomposition of DMAlH. Thermal rate coefficients in the high-pressure limit were calculated using conventional transition state theory (TST)[18] employing the POLYRATE program.[19] The rate coefficients for each reaction were calculated for temperatures in the range of 400−2000 K and then fitted to the Arrhenius form, $k(T) = A \exp(-E_a/kT)$. For the reactions considered here the calculated rate coefficients fit nicely to the Arrhenius expression with the exponent E_a typically falling within a few kilocalories of the saddle point barrier height, $E^{\ddagger}$, or the endothermicity. The reaction $(CH_3)_2AlH \leftrightarrow H_3CAlH + CH_3$ proceeds with a very small or no barrier (loose transition state) and is best treated with variational TST, which will be reported in a future study. The present results are obtained using a Gorin model,[22] employing the properties of the separated fragments as the transition state in the association reaction. We are unaware of other experimental or theoretical rate data in the literature.

Several groups have studied the dimerization of DMAlH.[2,3] We also did calculations for the DMAlH dimer and found a structure similar to that reported by Nakajima and Yamashita.[1] Our calculations were carried out with the DFT method using the B3LYP functional and the 6-31G basis set. The binding energy computed with this basis set is 25.6 kcal/mol as compared to 28.0 kcal/mol obtained by Willis and Jensen[3] with the 6-31G(d,p) basis set.

We also carried out DFT calculations for decomposition proceeding from the DMAlH dimer. For comparison we first carried out calculations for the lowest energy pathway for decomposition of the monomer using the same method. Table 8 shows the results for $M_2AlH \rightarrow MAlCH_2 + H_2$. Here the barrier is 93.0 kcal/mol with the 6-31G basis set and 87.6 kcal/mol with the 6-31G** basis set compared to the 71.1 kcal/mol from CCSD(T) with extrapolation to the basis set limit. Clearly polarization functions have a significant effect here. However, we did not include polarization functions in our studies of the decomposition of the DMAlH dimer. As we will see no low-energy pathways were found and hence the omission of polarization functions will not significantly affect the results.

Figure 4 and Table 9A show computed energetics for DMAlH dimer decomposition. The first step in this process is elimination of H_2 to give Al_2M_4. This can then rearrange to M_3Al + MAl. The barrier for the first step is 75 kcal/mol with respect to the

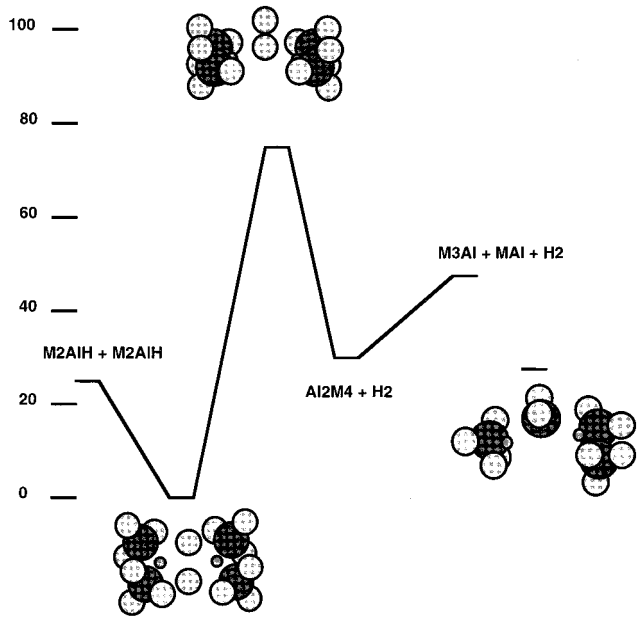

Figure 4. Energetics for DMAlH dimer decomposition.

TABLE 9: DFT Energy Differences

structure	ΔE, kcal/mol
A. For DMAlH Dimer Decomposition	
$MAlHCH_2 + M_2Al + H_2$	103.2
$M_3Al + MAl + H_2$	47.0
$Al_2M_4 + H_2$	29.2
sp3	75.3
$Al_2M_3HCH_2 + H_2$	26.7
$M_2AlH + M_2AlH$	25.7
$Al_2M_4H_2$, min2	35.4
$Al_2M_4H_2$	0.0
B. For DMAlH Bimolecular Reaction	
$M_3Al + MAl + H_2$	21.2
$Al_2M_4 + H_2$	3.4
$Al_2M_3HCH_2 + H_2$	0.9
$Al_2M_4-H_2$.sp	34.0
$M_2AlH + M_2AlH$	0.0

DMAlH dimer, or 18 kcal/mol lower than elimination of H_2 from DMAlH monomer at this level of calculation. Figure 4 and Table 9A also show an $Al_2M_3HCH_2$ structure with a bridging CH_2 group. This species could also be formed by elimination of H_2 from DMAlH dimer; however, we were not able to find the saddle point for this process. It is probable that $Al_2M_3HCH_2$ would decompose to $M_3Al + MAl$.

Table 9B gives energetics for the bimolecular reaction of two DMAlH molecules to give $Al_2M_4 + H_2$ and subsequent reactions of Al_2M_4. Here it is seen that the current calculations predict a barrier of 34.0 kcal/mol and an endothermicity of 21.2 kcal/mol to go to $M_3Al + MAl + H_2$.

Parts A and B of Table 10 show constrained pathways for removal of H_2 from the DMAlH dimer. Two pathways were defined relative to the plane containing the two Al and four C atoms of the DMAlH dimer. Both pathways move the midpoint of the H_2 bond perpendicular to the midpoint of the AlAl bond. Pathway 1 is in the plane, whereas pathway 2 is perpendicular to the plane. Pathway 2 leads to the saddle point shown in Figure 4, whereas pathway 1 leads to a higher barrier (~100 kcal/mol). In the case of pathway 1 the two Al and four C atoms remain coplanar, but in the case of pathway 2 the four C atoms are allowed to move to a pyramidal arrangement about the Al atoms. Pathway 2 is cleanly defined by a single reference configuration, but pathway 1 is a forbidden reaction that involves

TABLE 10: DFT Energy Differences (Kilocalories per Mole) for $Al_2M_4H_2 \rightarrow Al_2M_4 + H_2$

A. Path 1[a]

R,[b] au	short R[c]	long R[c]
0.5	7.7	
1.0	39.8	
1.5	95.0	101.0
2.0	149.1	66.7
3.0		44.4
$Al_2M_4H_2$, min	0.0	0.0

B. Path 2

R,[d] au	ΔE, kcal/mol
0.1	62.1
0.5	75.0
0.56 (sp)	75.3
1.0	61.7
$Al_2M_4H_2$, min	0.0

[a] The calculations in this table used the 6-31G* basis set. All other DFT calculations used the 6-31G basis set. [b] See text for description of the geometry. R is the distance between the midpoints of the AlAl bond and departing H_2 bond. [c] Short R calculation starts from the DMAlH geometry, whereas the long R calculation starts from the $Al_2M_4 + H_2$ geometry. See text. [d] See text for description of the geometry. R is the distance between the midpoint of the AlAl bond and closer H atom of the departing H_2.

a surface crossing where the two configurations differ by a double excitation. The latter process cannot be described by a single reference configuration and leads to two pathways that cross. The pathway starting from the DMAlH dimer is labeled by short R, and the pathway starting from $Al_2M_4 + H_2$ is labeled by long R.

From Figure 1 it is clear that the lowest energy pathway for decomposition of the DMAlH dimer is dissociation back to two monomers. Decomposition to $Al_2M_4 + H_2$ has a barrier of 80 kcal/mol at the CCSD(T) level with the cc-pVDZ basis set. This pathway is consistent with the experimental observation of trimethylaluminum as a product in Al CVD. However, given that Nakajima and Yamashita[1] determined that DMAlH is mostly monomer at higher temperatures and the first step of this reaction has a large barrier, it seems unlikely that this process is a major pathway in Al CVD.

IV. Conclusions

We have characterized the pathways for thermal decomposition of DMAlH using highly accurate ab initio methods [CCSD(T) with cc-pVnZ basis sets and MP2 extrapolation to the CBS limit] and have computed rate constants using the computed energetics and harmonic vibrational frequencies. We find that the lowest energy pathway leads to CH_3AlCH_2 with a barrier of 71.1 kcal/mol, which is below the first product resulting from direct bond breaking ($CH_3Al + CH_3$ at 82.2 kcal/mol). The pathway leading to $CH_3Al + CH_4$ has a barrier of 90.4 kcal/mol. From comparison studies of $AlH + H_2$ and $AlH + CH_4$ we conclude that the high barrier in the case of $CH_3Al + CH_4$ is very reasonable. [The singlet to triplet excitation energy in AlH is quite large (43.3 kcal/mol), which suggests low reactivity as a carbene for AlH.]

We also studied decomposition from the DMAlH dimer. However, the latter process has a relatively large barrier [~75 kcal/mol at the DFT/B3LYP/6-31G level and 80 kcal/mol at the CCSD(T) level with the cc-pVDZ basis set], and it seems unlikely that this process plays an important role in Al CVD.

Acknowledgment. This work was supported by NASA Contracts NAS2-14031 and NAS2-99092 to ELORET.

Supporting Information Available: Eleven tables containing total energies for all the calculations as well as geometries for all the stationary points are provided. This material is available free of charge via the Internet at http://pubs.acs.org.

References and Notes

(1) Nakajima, T.; Yamashita, K. *J. Mol. Struct.* **1999**, *490*, 155.

(2) Hiraoka, Y. S.; Mashita, M. *J. Crystal Growth* **1994**, *145*, 473.

(3) Willis, B. G.; Jensen, K. F. *J. Phys. Chem. A* **1998**, *102*, 2613.

(4) Becke, A. D. *J. Chem. Phys.* **1993**, *98*, 5648.

(5) Tachibana, A.; Sakata, K.; Omoto, K. *Appl. Surf. Sci.* **1997**, *117*, 465.

(6) Dunning, T. H., Jr. *J. Chem. Phys.* **1989**, *90*, 1007.

(7) (a) Kendall, R. A.; Dunning, T. H., Jr.; Harrison, R. J. *J. Chem. Phys.* **1992**, *96*, 6796. (b) Woon, D. E.; Dunning, T. H., Jr. *J. Chem. Phys.* **1993**, *98*, 1358.

(8) Hampel, C.; Peterson, K.; Werner, H.-J. *Chem. Phys. Lett.* **1992**, *190*, 1.

(9) Knowles, P. J.; Hampel, C.; Werner, H.-J. *J. Chem. Phys.* **1993**, *99*, 5219.

(10) Martin, J. M. L. *Chem. Phys. Lett.* **1996**, *259*, 669.

(11) Ricca, A.; Bauschlicher, C. W. *J. Phys. Chem.* **1998**, *102*, 876.

(12) Dunning, T. H., Jr.; Peterson, K. A. *J. Chem. Phys.* **2000**, *113*, 7799.

(13) Werner, H.-J.; Knowles, P. J. *J. Chem. Phys.* **1988**, *89*, 5803; Knowles, P. J.; Werner, H.-J. *Chem. Phys. Lett.* **1988**, *145*, 514.

(14) Langhoff, S. R.; Davidson, E. R. *Int. J. Quantum Chem.* **1974**, *8*, 61.

(15) DALTON, an electronic structure program, release 1.0, written by Helgaker, T.; Aa. Jensen, H. J.; Jørgensen, P.; Olsen, J.; Ruud, K.; Ågren, H.; Andersen, T.; Bak, K. L.; Bakken, V.; Christiansen, O.; Dahle, P.; Dalskov, E. K.; Enevoldsen, T.; Fernandez, B.; Heiberg, H.; Hettema, H.; Jonsson, D.; Kirpekar, S.; Kobayashi, R.; Koch, H.; Mikkelsen, K. V.; Norman, P.; Packer, M. J.; Saue, T.; Taylor, P. R.; Vahtras, O. 1997.

(16) MOLPRO, a package of ab initio programs written by Werner, H.-J. and Knowles, P. J., with contributions from Almlöf, J.; Amos, R. D.; Deegan, M. J. O.; Elbert, S. T.; Hampel, C.; Meyer, W.; Peterson, K.; Pitzer, R.; Stone, A. J.; Taylor, P. R.; Lindh, R. 1996.

(17) Gaussian 94, revision D.1. Frisch, M. J.; Trucks, G. W.; Schlegel, H. B.; Gill, P. M. W.; Johnson, B. G.; Robb, M. A.; Cheeseman, J. R.; Keith, T.; Petersson, G. A.; Montgomery, J. A.; Raghavachari, K.; Al-Laham, M. A.; Zakrzewski, V. G.; Ortiz, J. V.; Foresman, J. B.; Cioslowski, J.; Stefanov, B. B.; Nanayakkara, A.; Challacombe, M.; Peng, C. Y.; Ayala, P. Y.; Chen, W.; Wong, M. W.; Andres, J. L.; Replogle, E. S.; Gomperts, R.; Martin, R. L.; Fox, D. J.; Binkley, J. S.; Defrees, D. J.; Baker, J.; Stewart, J. P.; Head-Gordon, M.; Gonzalez, C.; Pople, J. A. Gaussian, Inc., Pittsburgh, PA, 1995.

(18) See, for example: Truhlar, D. G.; Isaacson, A. D.; Garrett, B. C. Generalized Transition State Theory. In *Theory of Chemical Reaction Dynamics*; Baer, M., Ed.; CRC Press: Boca Raton, FL, 1985; Vol. IV, pp 65−137. Gilbert, R. G.; Smith, S. C. *Theory of Unimolecular and Recombination Reactions*; Blackwell Scientific Publications: Oxford, U.K., 1990.

(19) Steckler, R.; Chuang, Y.-Y.; Coitiño, E. L.; Fast, P. L.; Corchado, J. C.; Hu, W.-P.; Liu, Y.-P.; Lynch, G. C.; Nguyen, K. A.; Jackels, C. F.; Gu, M. Z.; Rossi, I.; Clayton, S.; Melissas, V. S.; Garrett, B. C.; Isaacson, A. D.; Truhlar, D. G. POLYRATE, version 7.2; University of Minnesota, Minneapolis, MN, 1997.

(20) Peterson, K. A.; Werner, H.-J. *J. Chem. Phys.* **1992**, *96*, 8948.

(21) Walch, S. P.; Dateo, C. E. *J. Phys. Chem. A* **2001**, *105*, 2015.

(22) Gorin, E. *Acta Physiochim. USSR* **1938**, *9*, 691.